



International Journal of Control Theory and Applications

ISSN : 0974-5572

© International Science Press

Volume 10 • Number 10 • 2017

Serrated Circular Fractal Coplanar Wave Guide Fed Antennas for Wideband and Ultra Wideband Applications

¹D S Ramkiran, ²P Siddaiah and ³B T P Madhav

¹Research Scholar, Department of ECE, JNTUH, India

²Professor, Department of ECE, Acharya Nagarjuna University, AP, India

³Professor, Department of ECE, K L University, AP, India

Abstract: Circular fractal antenna and circular serrated fractal antenna are designed to operate in the wideband (2.9-13.1 GHz) and ultra wideband (3.1 to 10.6 GHz) range. Circular fractal antenna with slots in the radiating element is providing impedance bandwidth of 89% and bandwidth of 10.02 GHz in the operating band. Circular serrated fractal antenna is providing an impedance bandwidth of 84% and bandwidth of 8.86 GHz. The prototyped circular serrated fractal antenna is tested on ZNB-20 vector network analyzer and observed the similar results of HFSS. Both antennas are providing excellent radiation characteristics with considerable gain make these models suitable for S, C and X-band communication systems.

Keywords: Circular Fractal, Coplanar Wave Guide (CPW), Serrated Antenna, Wideband, Ultra Wideband (UWB).

1. INTRODUCTION

Research on ultra-wideband (UWB) has drawn wide interest from the researchers for increasing the data rate in wireless communication since federal Communication Commission (FCC) had allocated an unlicensed band from 3.1 GHz to 10.6 GHz for commercial use of high data rate wireless communication [1]. Being an essential part of ultra-wideband (UWB) system, UWB antennas have drawn wide interest for researchers. Recently, due to many attractive features like low profile, light weight and low cost printed monopole antennas are frequently used for UWB application [2-4]. These antennas should have a broad impedance bandwidth from 3.1 to 10.6 GHz, stability in radiation characteristics with good omni-directional pattern and compact in size. Additionally some frequency bands including World Interoperability for Microwave Access (WiMAX) system at 3.5 GHz (3.4-3.69 GHz), lower WLAN at 5.2 GHz (5.15-5.35 GHz), and higher WLAN at 5.8 GHz (5.725-5.825 GHz) and X-band downlink communication frequency at 7.5 GHz (7.1-7.76GHz) have been allocated within the designated ultra-wideband [5].

A new kind of slot structure radiating patch and co-ground structure made this antenna compact in size in comparison to various existing antennas. The hexagonal microstrip fractal antenna powered through CPW fed structure for ultra-wide band wireless communication applications has been reported in [6]. It was shown to have good impedance characteristics over an UWB frequency range from 3.1 to 10.6 GHz. A novel compact-

size CPW-fed UWB antenna with large bandwidth of 1.2 to 25 GHz has been investigated in [7]. This antenna consists of a circular disc, a spiral split ring resonator and CPW fed along with two tapered transmission lines for improving broadband impedance matching in the required band. In [8], inkjet-printing on MID technology for the realization of ultra-wide band antennas has been presented, which gives a good impedance matching over the entire ultra-bandwidth of 3 GHz–13 GHz. Jawad *et al.* have presented ultra-wideband antenna with complementary characteristics with the help of a pair of split ring resonators [9-10].

2. ANTENNA GEOMETRY

Circular fractal antenna and circular serrated fractal antenna are designed on FR4 dielectric material of permittivity 4.4. The design and simulation is performed on high frequency structural simulator tool as well as in CST microwave studio for validation. and presented in this work. The antenna dimensional values are presented in table 1 and the physical structure is presented in Fig 1 and Fig 2. The overall dimension of the antenna models

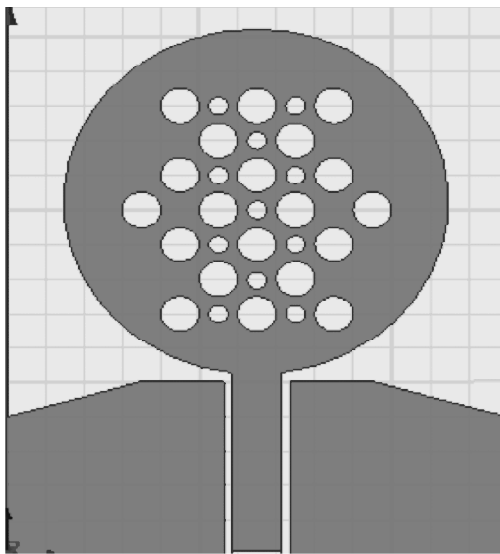


Figure 1: Circular Fractal Antenna

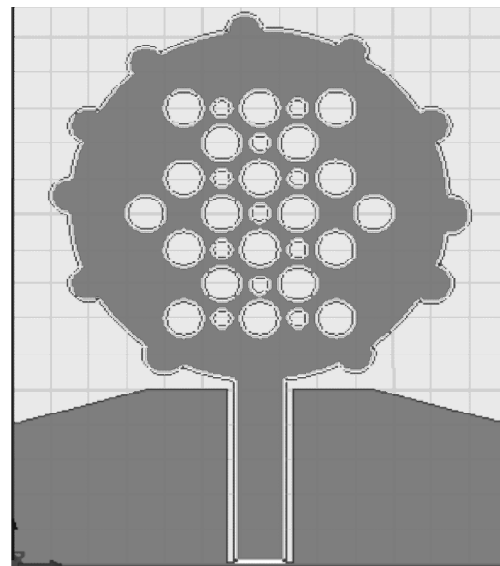


Figure 2: Circular Serrated Fractal

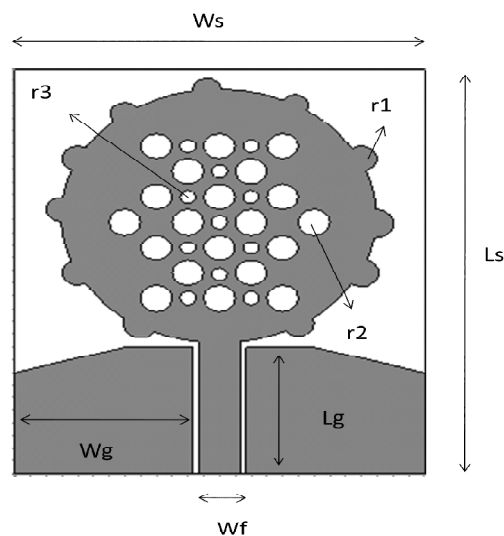


Figure 3: Serrated Fractal Antenna geometry

are around 31x26x1.6 mm. Circular slots are placed on the radiating element to get fractal geometry for model 1 and additional circular strips are added to the radiating element boundary to get serrated geometry in model 2. Coplanar waveguide feeding is used in both the models with feed line and ground plane gap of 0.3 mm for impedance matching.

Table 1
Antenna dimensions in mm

Parameter	W_s	L_s	W_g	L_g	W_f	$r1$	$r2$	$r3$
Dimension in mm	31	26	11.7	10	2.6	1.2	1	0.5

3. RESULTS AND DISCUSSION

The band width of an antenna is the range of frequencies within which the performance of the antenna with respect to some characteristic conforms to a specified standard. If the antenna impedance is matched to the transmission line at resonance, the mismatch off resonance is related to the voltage standing wave ratio. The value of VSWR which can be tolerated then defines the bandwidth of the antenna. If this value is less than s, the usable bandwidth of the antenna is related to the total Q-factor by

$$B = \frac{1}{Q} \frac{S-1}{\sqrt{S}} = \frac{VSWR-1}{\sqrt{VSWR} \cdot Q_T} \tag{1}$$

The designed antenna models are simulated using HFSS and CST and presented in this section. Circular fractal antenna reflection coefficient is presented in Fig 4. The result shows that antenna is working in the wide range from 2.9-13 GHz with bandwidth of 10 GHz. Circular serrated fractal antenna is working in the range of 3-11.9 GHz with bandwidth of 8.8 GHz . Model 1 is providing the impedance bandwidth of 80% and model 2 is providing 91%. The reflection coefficient of the serrated fractal antenna is also simulated with CST tool and observed that the bandwidth is improved by 0.1 %. An impedance bandwidth of 92% is attained from this solver.

The input impedance at the feed of the antenna is

$$Z = R + jX = \frac{V}{I} = \frac{-E_{avt}}{I} \tag{2}$$

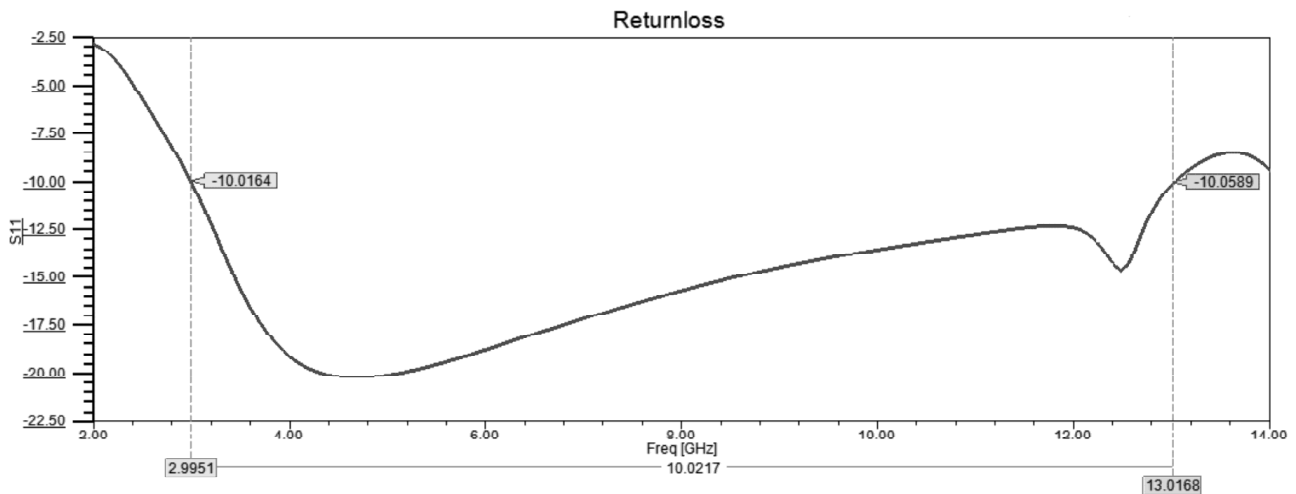


Figure 4: Simulated S11 of circular fractal antenna (HFSS)

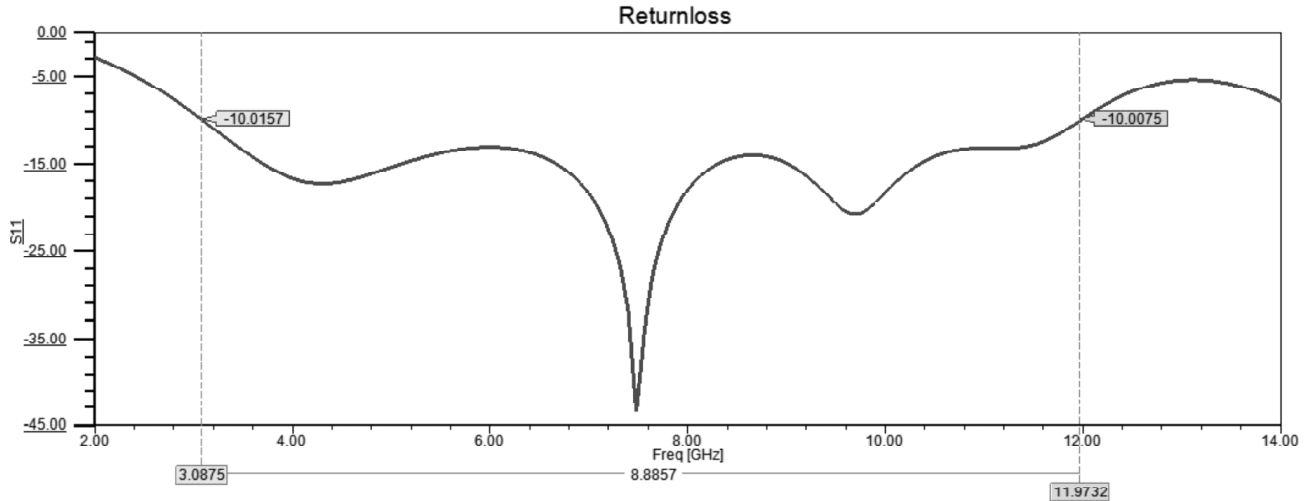


Figure 5: Simulated S11 of Serrated Fractal Antenna (HFSS)

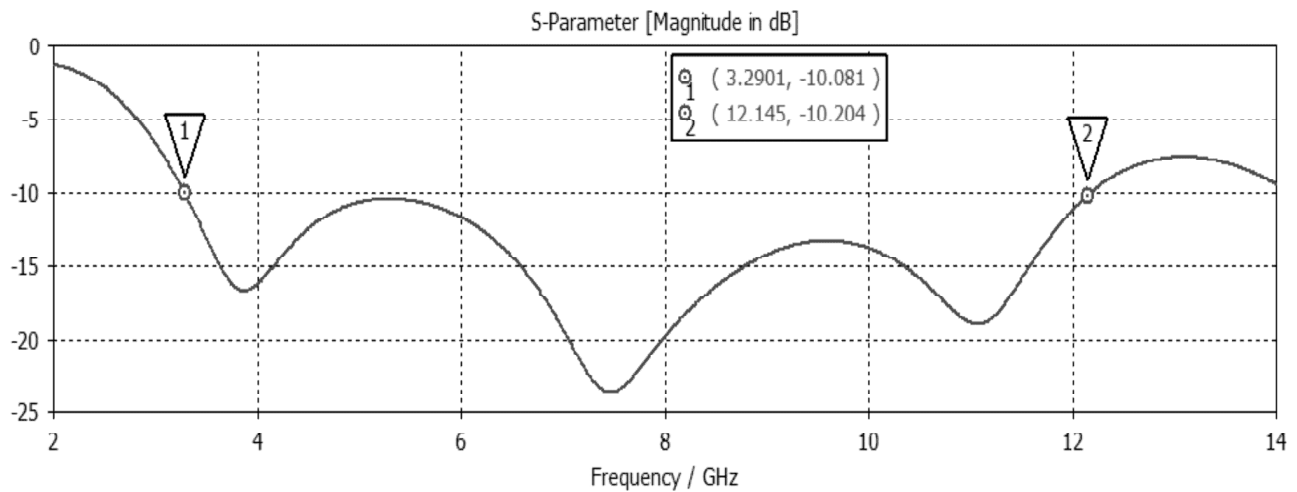


Figure 6: Simulated S11 of Serrated Fractal Antenna (CST)

Where E_{av} is the average value of the electric field at the feed point and I is the total current.

The input impedance is complex and involves a resistive and reactive part. The resistive and reactive components vary as a function of frequency and are symmetric around the resonant frequency.

For a probe fed circular patch, the input impedance with near resonance can be represented as a function of frequency and feed location as,

$$Z_{in}(f, P) = R_{in}(f, P) + jX_{in}(f, P) \quad (3)$$

The input resistance at resonance varies with radial distance P from the centre of the patch as,

$$R_{in}(f = f_r, nm, P) = R_r(P) = \frac{R_{edge} J_n^2(kP_o \frac{a}{nm})}{J_n^2(ka)} \quad (4)$$

The input impedance of a rectangular patch and feed location expressed as the functions of frequency and feed location (x_o, y_o) as,

$$Z_{in}(f, x_o) = R_{in}(f, x_o) + jX_{in}(f, x_o) \tag{5}$$

The impedance characteristics of the serrated antenna determined from CST tool and presented in Fig 7. An average impedance of 40 ohms is attained in the operating band of the serrated antenna.

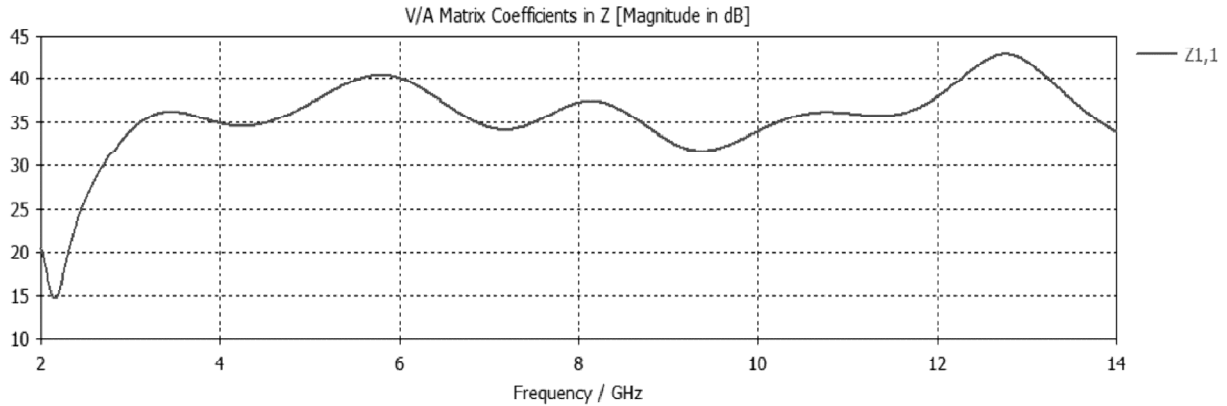


Figure 7: Impedance Vs Frequency of Serrated Fractal Antenna (CST)

For each mode, there are two orthogonal planes in the far field region. One designated as E-plane and the other designated as H-plane. The far zone electric field lies in the E-plane and the far zone magnetic field lies in the H-plane. The patterns in these planes are referred to as the E and H plane patterns respectively.

For the TM_{01} mode, the contributions to the far fields are from the magnetic surface current densities on the side walls containing the radiating edges. The directions of the magnetic currents that the E-plane is the y-z plane ($\Phi=90^\circ$) and the H-plane is the x-z plane ($\Phi=0^\circ$). For the TM_{10} mode, the E-plane is the x-z plane ($\Phi=0^\circ$) and the H-plane is the y-z plane ($\Phi=90^\circ$)

$$E_\theta(r, \theta, \phi) = -2wh \left(\frac{E_0}{\eta_0} \right) \cos \phi (1 - T^{TM}(\theta)) \cos \left(k_x \frac{L}{2} \right) \sin c \left(k_y \frac{w}{2} \right) \text{tanc}(k_z h)$$

$$E_\phi(r, \theta, \phi) = 2wh \left(\frac{E_0}{\eta_0} \right) (\cos \theta \sin \phi) (1 - T^{TE}(\theta)) \cos \left(k_x \frac{L}{2} \right) \sin c \left(k_y \frac{w}{2} \right) \text{tanc}(k_z h) \tag{6}$$

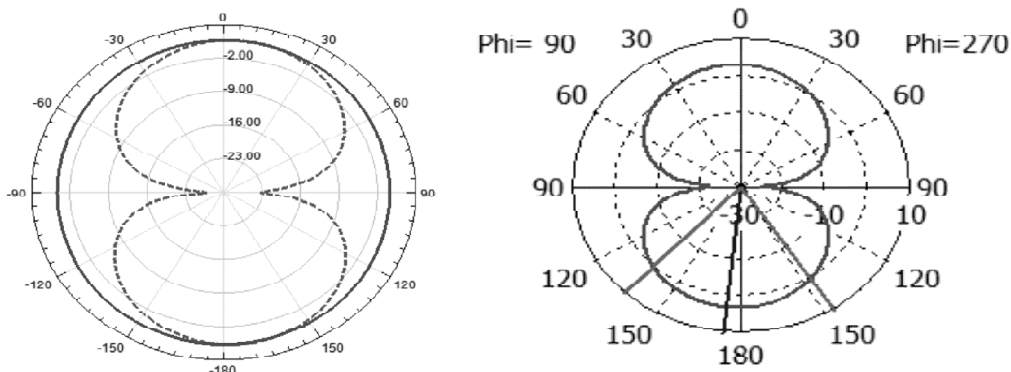


Figure 8: Radiation pattern of circular serrated fractal in HFSS & CST at 4.2 GHz

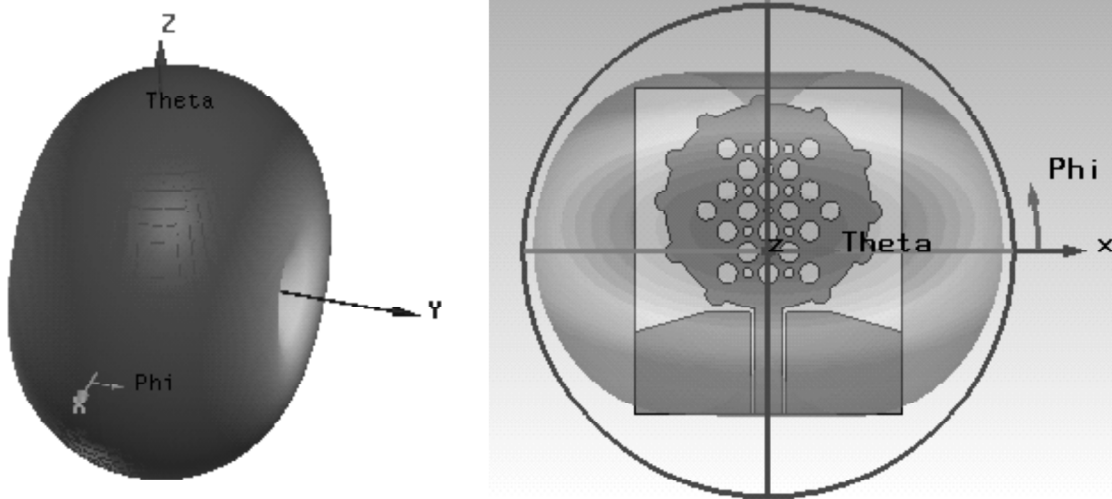


Figure 9: Three dimensional view of radiation at 4.3 GHz in HFSS and in CST

The radiation patterns of circular serrated fractal in HFSS and in CST are presented in Fig 8. The three dimensional view is presented in Fig. 9.

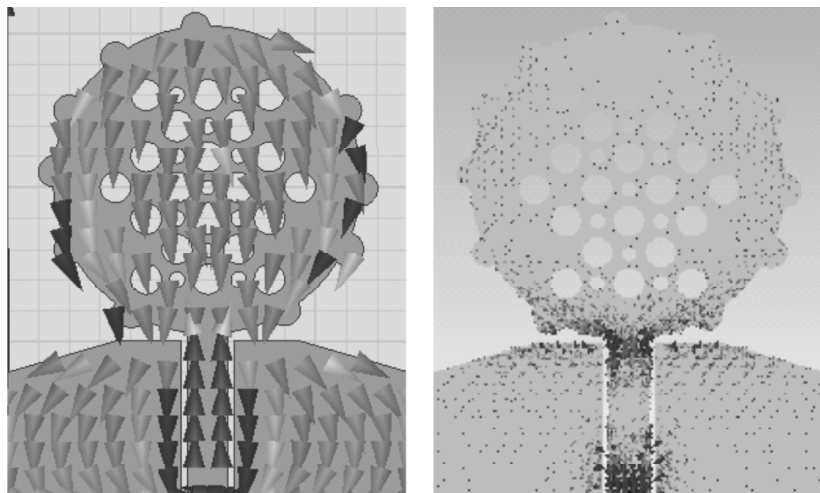


Figure 10: Current distribution on the surface of circular serrated antenna in HFSS & CST at 4.3 GHz

Antenna is showing peak realized gain of more than 5.2 dB in the operating band. The surface current distribution of the antenna at 4.3 GHz is presented in Fig 10. The current density is more focussed at feed line rather than radiating element. The distribution over the patch is also at edges only and the intensity around the slots is very low.

Fig 11 shows the normalized source and received pulses for circular serrated antenna model. The pulse fidelity values are larger than 0.5, which gives acceptable range for the case of wideband antennas. Fig 12 shows the measured reflection coefficient of the proposed antenna model prototyped on FR4 substrate. A 50 ohm sma connector is connected at port and S11 parameter is measured on ZNB 20 vector network analyzer. The simulation and measurement are in good agreement with each other. The prototyped antenna also can be observed form the measured return loss curve.

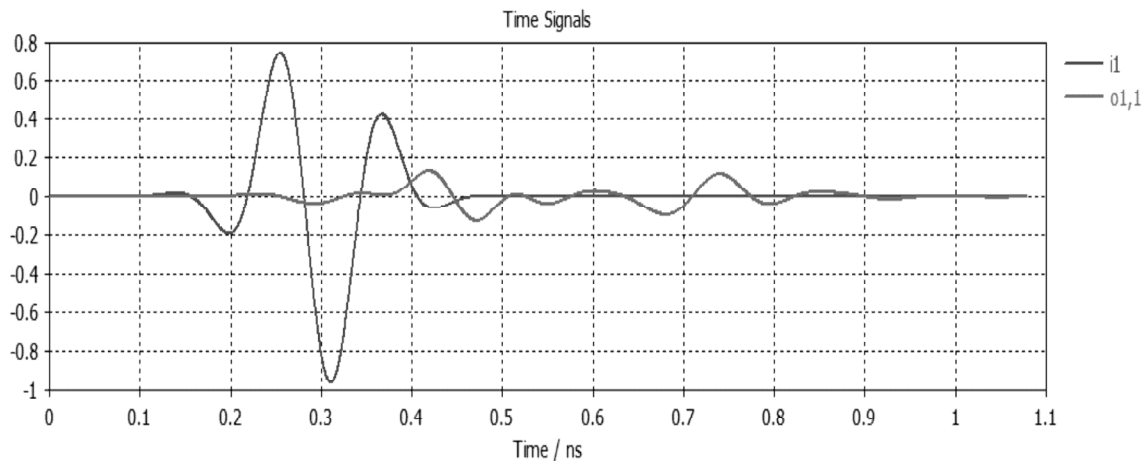


Figure 11

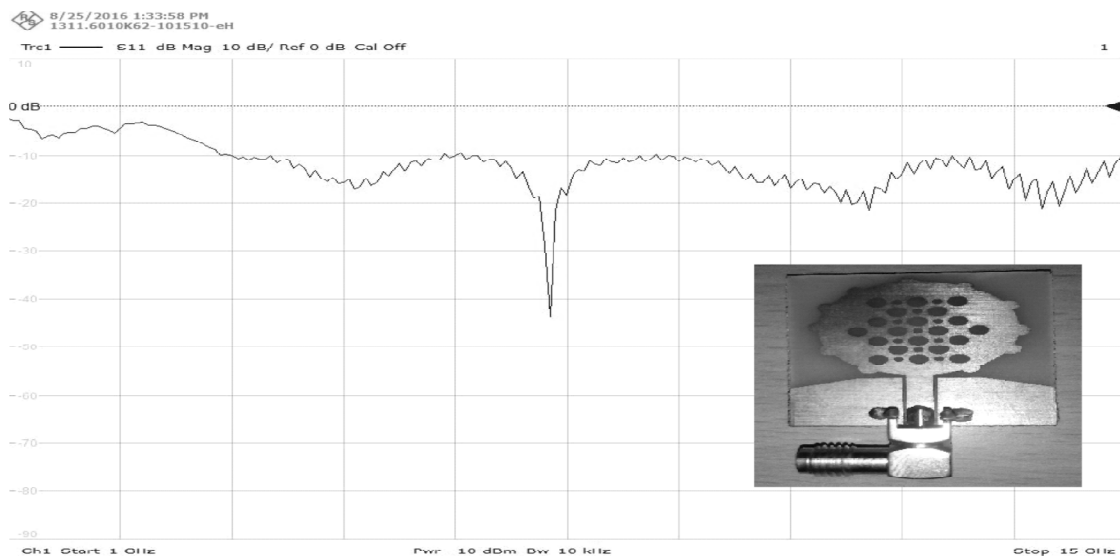


Figure 12: Measured S11 of prototyped antenna on ZNB 20 VNA

CONCLUSION

Two antenna models are designed for wideband communication systems. Circular fractal antenna is working in the wide range from 2.9-13 GHz with bandwidth of 10 GHz. Circular serrated fractal antenna is working in the range of 3-11.9 GHz with bandwidth of 8.8 GHz. Model 1 is providing the impedance bandwidth of 80% and model 2 is providing 91%. Circular serrated antenna is prototyped on FR4 substrate and measured results are collected from vector network analyzer for validation. In the time domain analysis the pulse fidelity values are larger than 0.5, which gives acceptable range for the case of wideband antennas. The measured and simulated results are showing good agreement and the radiation characteristics are good enough to place the current current in the communication band applications.

ACKNOWLEDGEMENTS

Authors are thankful to the department of ECE of K L University and ANU for the support during this work. Authors like to acknowledge the grant from DST to KLU through ECR / 2016/000569 and SR/FST/ETI-316/2012.

REFERENCES

- [1] M. Naghshvarian-Jahromi, "Novel miniature semi-circular-semifractal monopole dual band antenna," *J. Electromagn. Wave Applicat.*, JEMWA, vol. 22, pp. 195–205, 2008.
- [2] Ansoft High Frequency Structure Simulation (Ansoft HFSS v10.0) Ansoft Corporation, 2005.
- [3] CST Microwave Studio, Computer Simulation Technology 2008.
- [4] N. Behdad and K. Sarabadani, "A compact antenna for ultrawideband applications," *IEEE Trans. Antennas Propag.*, vol. 53, no. 7, pp. 2185–2192, 2005.
- [5] G. F. Tsachtsiris, C. F. Soras, M. P. Karaboikis, and V. T. Makios, "Analysis of a modified Sierpinski gasket monopole antenna printed on dual band wireless devices," *IEEE Trans. Antennas Propag.*, vol. 52, no. 10, pp. 2571–2579, 2004.
- [6] M. V. Reddiah Babu, Sarat K. Kotamraju, B. T. P. Madhav, COMPACT SERRATED NOTCH BAND MIMO ANTENNA FOR UWB APPLICATIONS, *ARNP Journal of Engineering and Applied Sciences*, ISSN 1819-6608, VOL. 11, NO. 7, APRIL 2016, pp 4358-4369.
- [7] K V L Bhavani, Habibulla Khan, D Sreenivasa Rao, B T P Madhav, Dual Band Notched Planar Printed Antenna with Serrated Defected Ground Structure, *Journal of Theoretical and Applied Information Technology*, ISSN: 1992-8645, Vol 88, Issue 1, June 2016, pp 28-34.
- [8] B T P Madhav, VGKM Pisipati, Habibulla Khan, D Ujwala, "Fractal shaped Sierpinski on EBG structured ground plane", *Leonardo Electronic Journal of Practices and Technologies*, ISSN 1583-1078, Issue 25, July-December 2014, pp 26-35.
- [9] S.S. Mohan Reddy, P. Mallikarjuna Rao, B.T.P. Madhav, Partial Substrate Removal Techniques for the Enhancement of Gain and Radiation Characteristics in Fractal Antenna, *Research Journal of Applied Sciences, Engineering and Technology*, ISSN: 2040-7459, Vol 10, Issue 1, May 2015, pp 79-85.
- [10] B T P Madhav, K Sai ram, M Deepika, V Naresh, "Circularly Polarized Koch Fractal Triband Antenna for Communication Applications" *ARNP Journal of Engineering and Applied Sciences*, ISSN: 1819-6608, Vol 10, No 14, Aug-15, pp 5795-5801.